

Integrating Cybersecurity in Predictive Cost-Benefit Power Scheduling: A DeepStack Model with Dynamic Defense Mechanism

Ali Peivand, Seyyed Mostafa Nosratabadi, *Member, IEEE*

Abstract—This paper introduces a novel, deep learning-based predictive model tailored to address wind curtailment in contemporary power systems, while enhancing cybersecurity measures through the implementation of a Dynamic Defense Mechanism (DDM). The augmented BiLSTM architecture facilitates accurate short-term predictions for wind power. In addition, a ConvGAN-driven step for stochastic scenario generation and a hierarchical, multi-stage optimization framework, which includes cases with and without Battery Energy Storage (BES), significantly minimizes operational costs. The inclusion of DDM strategically alters network reactances, thereby obfuscating the system's operational parameters to deter cyber threats. This robust solution not only integrates wind power more efficiently into power grids, leveraging BES potential to improve the economic efficiency of the system, but also boosting the cyber security of the system. Validation using the Illinois 200-bus system demonstrates the model's potential, achieving a 98% accuracy in forecasting and substantial cost reductions of over 3.8%. The results underscore the dual benefits of enhancing system reliability and security through advanced deep learning architectures and the strategic application of cybersecurity measures.

Index Terms—Deep-aided optimal scheduling, Dynamic Defense Mechanisms, GAN-driven stochastic scenarios, Power system scheduling, Wind curtailment.

NOMENCLATURE

A. Indices

| | |
|------|--|
| t | Time index |
| b | Battery Energy Storage index |
| n | Generator index |
| WF | Wind farm index |
| d | Discriminator component index of the GAN model |
| g | Generator component index of the GAN model |
| L | Neural Network Layers |
| i | Attack vector in DDM model |

B. Parameters

| | |
|-------------------------|---|
| Pr_n^{su}, Pr_n^{sd} | Price of start-up and shutdown for n^{th} generator |
| S_b^{ch}, S_b^{dis} | Charge and discharge price of battery energy storage |
| η_{ch}, η_{dis} | Charge and discharge efficiency |

| | |
|-------------------------|---|
| A | Incidence matrix |
| H_t | Measurement matrix at time t |
| C. Variables | |
| C_{ss} | Start-up and shutdown costs |
| C_f | Generator fuel costs |
| C_w | Wind farm operating costs |
| C_b | Battery energy storage cost |
| p_n^t | Scheduled power of n th generator at time t |
| P_{ch}^t, P_{dis}^t | Charging and discharging power of energy storage |
| E_b^t | Energy level of energy storage at time t |
| α_n^t, β_n^t | On and Off states of n th generator at time t |
| η | Success rate of attack detection |
| D_l | Diagonal matrix of the reciprocals of branch reactances |
| $x_{l,t}$ | Reactance of line l at time t |

I. INTRODUCTION

THE modern power system has experienced significant transformations in recent years, driven by efforts to minimize operating costs and optimize other key performance characteristics. However, the increasing integration of wind power has introduced several challenges for power grids. The intermittent nature of wind generation leads to a consistent risk to the reliability and stable operation of the system. This variability not only threatens grid security but also increases total costs and strains reserve capacities. With the accelerating cost reduction in wind power—falling by over 35% between 2010 and 2021 [1]—investments in wind farms are expected to continue growing. Despite this, challenges remain, as demonstrated by Spain curtailing over 1100 GWh of wind energy in 2013. In this way, well-structured optimization frameworks can potentially dwindle wind power curtailment as China's wind curtailment decreased from 17% in 2016 to 3% by 2020 [2].

Recent advancements in Artificial Intelligence (AI), particularly in neural networks, have paved the way for more effective optimization and predictive modeling. Traditional statistical methods often provide only rough estimations, which are insufficient for high-dimensional and complex datasets, as they struggle to capture the intricate hidden relationships

(Corresponding author: Seyyed Mostafa Nosratabadi).

Ali Peivand is with the Department of Electrical and Computer Engineering, Golpayegan College of Engineering, Isfahan University of Technology, Golpayegan, Iran (e-mail: alipeivand1376@gmail.com).

Seyyed Mostafa Nosratabadi is with the College of Engineering and Physical Sciences, University of Birmingham, Edgbaston, Birmingham, B15 2TT, UK (e-mail: s.m.nosratabadi@bham.ac.uk).

among observations. Hence, statistical models, such as Auto-regressive Integrated Moving Average (ARIMA) or seasonal-ARIMA models [3], were replaced with AI-aided models and techniques to perform regression and estimation based on a large amount of historical data. One of the primary applications of AI in power systems is forecasting, which enables more cost-effective and efficient exploitations. Accurate day-ahead estimation and prediction can promote and guarantee optimal scheduling and can be a system operator supporter, which are achievable by modified AI-based techniques such as Machine Learning (ML) and Deep Learning (DL). Learning-based methods have a vast utilizations in power system optimization, ranging from curtailment and optimal power flow prediction [4, 5] to congestion management [6]. Depending on the nature of each model, some recurrent-based ML methods surpass in time-series prediction task, for instance wind power. In contrast to weak ML techniques, deep-based methods result in higher accuracy and efficiency, as it is proven by authors in [7] that employs a robust-to-outliers LSTM model to predict wind power, aiding signal decomposition techniques. Hybrid combination can even more diminish the prediction error, exploiting learnable features of observations. For instance, in [8], the probabilistic-based prediction by Convolutional Neural Network (CNN) and LSTM gains superiority in comparison with single LSTM utilizing.

Apart from wind forecasting, DL models can enhance the performance of energy storage systems in various ways, including sizing estimation and optimizing operational tasks. Recent studies have investigated prediction and estimation models for Battery Management Systems (BMSs), with a strong focus on using artificial neural network (ANN)-based optimization for Battery Energy Storage (BES) [9]. In [10], a forecasting LSTM-designed model empowered by genetic algorithm is used to tackle with renewable energy uncertainty and energy storage sizing. One of the key technical parameters of energy storage systems is the state of charge (SOC), a continuous variable that is crucial for optimal scheduling. Moreover, authors in [11], utilizing the CNN-LSTM method, investigate state-of-charge (SOC) estimation which can be crucial for reliability. The importance of energy storage resources in reducing costs, losses, and wind power interruptions [12], combined with the powerful capabilities of deep learning models, has motivated many studies to integrate these two factors for power system optimization. In [13], charging and discharging optimal scheduling are determined by a deep Q-network structure. Prediction and optimization of energy storage along with other power system participants ensure maintaining reliable and stable operation of power system. In [14], a hybrid predictive model is considered which aims to forecast SOC and renewable energy resource power. Moreover, authors in [15] leverage the strength of the LSTM structure in predicting the charging levels of EV batteries. Additionally, a multi-feature training approach not only enhances learning efficiency but also achieves multiple objectives simultaneously.

Despite the noteworthy strides in integrating BES systems and the application of DNNs to enhance their operational efficiency, the landscape of modern power systems is marked by evolving challenges that necessitate rigorous and expansive research. This is particularly critical when endeavoring to harmonize

economic gains with burgeoning cybersecurity demands. When it comes to smart grids, the State Estimation (SE) plays a decisive role in detection of False Data-Injection (FDI) [16]. The incorporation of Dynamic Defense Mechanisms (DDM) ushers in a transformative layer of sophistication and utility, significantly augmenting system resilience. By dynamically modifying network parameters, DDM obscures the predictability of the system's operational state, thereby complicating the efforts of potential cyber attackers and reinforcing the overall security framework [17]. For instance, authors in [18] employed a Moving-Target Defense (MTD) model which aims to constantly alter the lines' reactances, distorting attackers' information about the system. The symbiotic relationship between DDM and BES transcends conventional benefits, serving a dual purpose: it substantively bolsters the physical robustness of the power infrastructure and shields it against cyber threats. This dual strategy not only mitigates operational costs and reduces instances of power curtailment but also enhances the grid's ability to withstand and adapt to disruptions, thereby elevating its overall resilience [19]. The combination of these technologies ensures a fortified defense against both physical failures and cyber intrusions, establishing a more reliable and secure grid environment. Despite numerous studies investigating BES and DNN's impact on power system efficiency, several critical research gaps remain:

- A scarcity of studies bridging cost-efficient and cybersecurity-based optimization frameworks, particularly those leveraging a DeepStack model incorporating BiLSTM for forecasting and ConvGAN for scenario generation.
- Limited investigation of BES impacts within economic and cybersecurity optimization frameworks.
- Insufficient predictive analysis aimed at reducing wind curtailment while simultaneously enhancing cybersecurity.

Addressing these challenges, our model proposes a dual strategy integrating advanced predictive analytics with robust cybersecurity measures to not only enhance grid stability but also reduce vulnerability to cyber-attacks. Briefly, the main contributions of the proposed model are as follows:

- Development of a DeepStack BiLSTM-CNN model to predict both cost-benefit optimal scheduling and cybersecurity-guaranteeing solutions in the power system, investigating two case studies: with and without BES.
- Proposing a learning-driven, multi-feature optimization framework utilizing an enhanced BiLSTM architecture for precise wind power forecasting.
- Application of Convolutional GANs (ConvGANs) to accurately model wind power fluctuations, significantly improving the reliability of simulation outcomes.

The remainder of this paper is organized as follows: The methodology section outlines the overall optimization procedure of the proposed model. The third section presents the results and outcomes of each stage. Finally, the conclusion is provided in the last section.

II. METHODOLOGY

The overall procedure of the proposed model is demonstrated in this section. As mentioned, this paper proposes a hierarchy multi-stage framework to predict the optimal scheduling of a power system including BES. The overall detailed workflow of the proposed model is demonstrated in Fig. 1. The workflow begins with gathering essential data, including features such as wind power and capacity, which undergo advanced preprocessing using machine learning-based imputation techniques to handle missing values. Following this, an

enhanced BiLSTM model predicts short-term wind power by capturing temporal patterns, enhancing prediction accuracy. ConvGAN is then applied to model fluctuations and generate synthetic scenarios, simulating diverse wind power generation conditions. This leads to the optimization phase, where two separate optimization frameworks (economic-based and security-based) are considered under two cases—one with Battery Energy Storage (BES) and one without—are modeled using Pyomo-enabled Mixed-Integer Nonlinear Programming (MINLP) to determine the optimal scheduling of power resources [20].

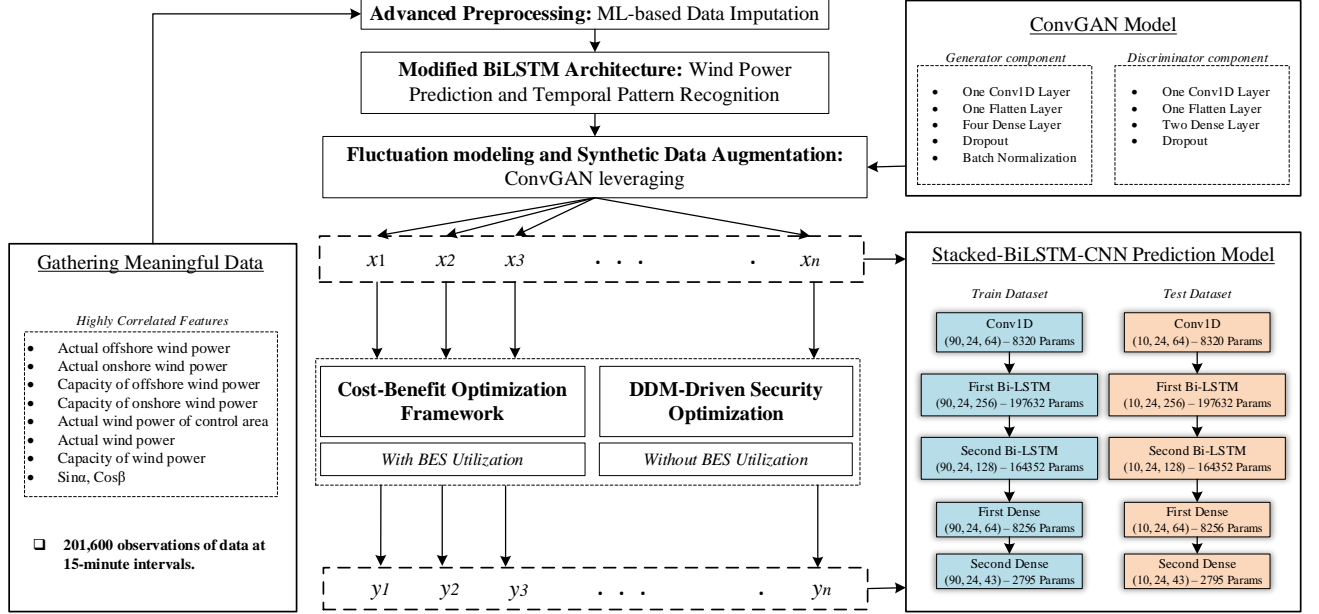


Fig. 1. Detailed workflow of the proposed model: integrating cost-efficient and security-based optimization framework.

Finally, a stacked BiLSTM-CNN model evaluates the predictive performance on training and testing datasets, demonstrating the effectiveness of this integrated deep learning and optimization approach in reducing wind curtailment and improving economic efficiency in power systems.

1) *Data Recovery*: The data retrieval is carried out by a Random Forest (RF) regressor, as an ensemble ML-based method. This estimator utilizes multitude trees to fit on training data sets, ending up with enhancing the prediction performance and escaping overfitting. When it comes to comparing RF to other likely ML-based methods, RF's robustness to noise, being computational costly efficient, and its interpretability makes it more appropriate, especially for an important task like missing data handling. While it starts randomly bagging observations, as binary splitting, from the first tree, and ultimately reaching terminal nodes, its cost function is computed as the averaging all trees. In other words, the final prediction is reliant on the averaging for regression. To check the convergence, the generalization error should be calculated as:

$$PE^* = P_{x,y}[mg(X,Y) < 0] \quad (1)$$

Where $mg(X,Y)$ is the margin function, defining in Eq. (2). Also, X and Y are the distribution of random vectors [20].

$$mg(X,Y) = av_k I[h_k(X, \Theta_k) = Y] - \max_{j \neq Y} av_k I[h_k(X, \Theta_k) = j] \quad (2)$$

In Eq. (2), Θ_k represents independent identically distributed random vectors in which $k = \{1,2,3, \dots, K\}$. Moreover, $av(\cdot)$ and $I[\cdot]$ are as average and indicator, respectively.

2) *Wind Power Prediction*: An advanced BiLSTM model is employed for short-term wind power prediction. This study also compares the proposed model with alternative prediction models to identify the most suitable approach. Conventionally, some recurrent-based methods such as LSTM is considered to forecast time-dependent variables, in this case wind power [21]. However, some shallow and naïve utilization of these methods often impede their ability to fully capture the hidden relationships between observations.

To enhance time-series modeling, particularly in wind power prediction, this paper proposes an optimized BiLSTM model. The BiLSTM architecture not only retains the LSTM's capability to filter out irrelevant information through its forget gate but also effectively addresses the issue of gradient decay, which is a common problem in traditional methods like LSTM,

GRU, and RNNs. Unlike standard LSTM, the BiLSTM model processes data in both forward and backward directions, allowing it to extract valuable information from both past and future contexts. This bidirectional processing enriches the learning process and mitigates the vanishing gradient problem to a certain extent [22]. Eqs. (3) to (10) represent the underlying equations of the BiLSTM model [23]. Eq. (3) represents the input gate, controlling the extent to which a new data point enters the cell.

$$i_l^t = \text{sigmoid}_{\text{ig}}^t (U_{li}^t \cdot h_l^{t-1} + W_{li}^t \cdot x_l^t + \theta_{li}) \quad (3)$$

Eqs. (4) and (5) formulate the forget and output gates, the former decides the amount of previous cell state to retain, and the latter determines the part of the cell state to output.

$$f_l^t = \text{sigmoid}_{\text{fg}}^t (U_{lf}^t \cdot h_l^{t-1} + W_{lf}^t \cdot x_l^t + \theta_{lf}) \quad (4)$$

$$O_l^t = \text{sigmoid}_{\text{og}}^t (U_{lo}^t \cdot h_l^{t-1} + W_{lo}^t \cdot x_l^t + \theta_{lo}) \quad (5)$$

Moreover, cell state update, shown in Eq. (6), generates a new candidate cell state, and final cell state is achieved by blending the old state and the new candidate state, according to Eq. (7).

$$\tilde{C}_l^t = \text{tanh}_{\text{ic}}^t (U_{lc}^t \cdot h_l^{t-1} + W_{lc}^t \cdot x_l^t + \theta_{lc}) \quad (6)$$

$$C_l^t = (f_l^t \otimes C_l^{t-1}) + (i_l^t \otimes \tilde{C}_l^t) \quad (7)$$

Where the W_l^t denotes the feed-forward weights, the θ_l is the bias vector, and the \tilde{C}_l^t is the cell state. Further, the i_l^t and O_l^t are input and output, respectively.

$$h_l^t = O_l^t \otimes (\text{tanh}_{\text{ic}}^t \cdot C_l^t) \quad (8)$$

$$\hat{y}_t = W_{yh} \cdot h^t + \theta_0 \quad (9)$$

$$\min \{L(y, \hat{y}_t)\} \quad (10)$$

In the BiLSTM structure, two back-and-forth channels have been provided which led to an increase in the learning rate even if data was insufficient. In other words, the output of the BiLSTM includes the forward h_l^t and backward $h_{backward,l}^t$ as formulated in Eqs. (8) and (9). Also, the objective function of the BiLSTM structure is to minimize the difference between real and predicted outputs, as illustrating in Eq. (10).

3) *Performance Evaluation*: The OPTUNA [24] optimizer is employed here to adjust the hyperparameters of DNN's model. In terms of performance assessment, some prevalent evaluation metrics have been used which are defined as follows:

$$MSE = \frac{1}{N} \sum_{j=1}^N (y_j^t - y_j^p)^2 \quad (11)$$

$$NRMSE = \frac{100 \sqrt{MSE}}{y_j^{\text{max}}} \quad (12)$$

$$MAPE = \frac{100 \sum_{j=1}^N |y_j^t - y_j^p|}{N} \quad (13)$$

where y_j^t and y_j^p indicate the target and prediction values of j^{th} observation in the mentioned data frame. Moreover, N refers to the total number of observations which is 201600 samples.

4) *ConvGAN Model*: In the power system optimization context, it is usual to implement proposed optimization model to a significant range of scenarios, assuring of the authenticity

and validity of the model. In this way, some random-based methods have been vastly utilized in order to generate synthetic data. Although the main positive side of these methods is their simplicities, they would not be reliable in case of high precision. To generate a synthetic data set which is highly similar to the original data set, some pioneer methods such as Auto Encoder Decoder (AED) and Generative Adversarial Network (GAN) can be applied. Accordingly, this paper outlines a convolutional-based structure for the GAN model, ConvGAN for short, which is practicable in learning complex patterns and generating synthetic data set with the highest similarities. The objective function of ConvGAN model is defined in Eq. (14). As the GAN model contains two opponent components, the generator and discriminator, its objective function embodies two terms, representing generator and discriminator error values [25].

$$\max_d \min_g \Theta(d, g) = \left\{ \begin{array}{l} E_{x \sim p(x)} [\log d_x] + \\ E_{z \sim p(z)} [\log(1 - d_x(g_z))] \end{array} \right\} \quad (14)$$

5) *Objective function of Model*: In this part, two considered case studies along with their objective functions and constraints are provided. All so far outcomes will be utilized in power system optimization through two cases with and without Battery Energy Storage (BES) system integration.

6) *Case1*: Firstly, the power system optimization is carried out without considering BES, indicated in Eq. (15), and includes generator and wind farm costs. Also, the costs related to the generators consist of two parts which are start-up and shutdown along with fuel costs.

$$F = \min \{C_{ss} + C_f + C_w\} \quad (15)$$

In Eq. (16) start-up and shutdown costs are formulated, using two binary variables, α_n^t and β_n^t , represented start-up and shutdown occurrences for n^{th} generator at time t . Additionally, Pr_n^{su} and Pr_n^{sd} are their corresponding cost coefficients.

$$C_{ss} = \sum_{t=1}^T \sum_{n=1}^N (Pr_n^{su} \alpha_n^t + Pr_n^{sd} \beta_n^t) \quad (16)$$

In Eq. (17), the quadratic form of fuel costs related to the generators are defined. Accordingly, the generator's cost coefficients are denoted by a_n , b_n , and c_n . In the Eq. (18), λ represents the coefficient price of each megawatt generated wind power based on the $\frac{\$}{MWh}$, and its value is 0.0001.

$$C_f = \sum_{t=1}^T \sum_{n=1}^n (a_n (p_n^t)^2 + b_n (p_n^t) + c_n) \quad (17)$$

$$C_w = \sum_{t=1}^T \sum_{w=1}^{WF} \lambda p_w^t \quad (18)$$

Furthermore, in Eqs. (19) to (21), the relations of the three binary variables used for generators operation modelling are observable where u_n^t assigns for the current state of each generator.

$$u_n^t - u_n^{t-1} \leq \alpha_n^t \quad \forall n \in N, t \in T \quad (19)$$

$$u_n^{t-1} - u_n^t \leq \beta_n^t \quad \forall n \in N, t \in T \quad (20)$$

$$\alpha_n^t + \beta_n^t \leq 1 \quad \forall n \in N, t \in T \quad (21)$$

7) *Case 2*: In the second case, power system optimal scheduling is determined considering BES integration which

can expect to contribute the cost and curtailment decrease. The corresponding objective function can be updated by Eq. (22), appending operating costs for energy storage, denoted by C_b .

$$F = \min \{C_{ss} + C_f + C_w + C_b\} \quad (22)$$

$$C_b = \sum_{t=1}^T \sum_{b=1}^B (S_b^{ch} P_{ch}^t + S_b^{dis} P_{dis}^t) \quad (23)$$

where S_b^{ch} and S_b^{dis} are charging and discharging battery price parameters. The energy level of the BESs can be calculated using Eq. (24), which accounts for the charging and discharging efficiencies, denoted by η_{ch} and η_{dis} , respectively. These efficiencies are set to 0.95.

$$E_b^t = E_b^{t-1} + \eta_{ch} P_{ch}^t - \frac{P_{dis}^t}{\eta_{dis}} \quad (24)$$

To ensure the feasible operation of the BESs, two mandatory constraints, defined by Eqs. (25) and (26), are imposed. These constraints guarantee that the storage operates within its capacity and power limits.

$$p_b^{\min} \leq p_{ch}^t, p_{dis}^t \leq p_b^{\max} \quad (25)$$

$$E_b^{T_{initial}} = E_b^{T_{final}} \quad (26)$$

The highest power capacity for a single battery is 250 MW, and with three batteries in the system, the total capacity reaches 750 MW. The constraints ensure that the BESs operate safely and efficiently while adhering to system limitations.

8) *DDM-related Equations*: In this section, some pivotal principles of equations related to the DDM are formulated. As previously explained, the main aim of this strategy is to constantly change the line reactances using adequate D-FACTS equipment installed on specific branches. This modification is intended to disrupt attackers' knowledge about the state of the system. To achieve this, a perturbation vector is added to the reactance matrix. This vector must be large enough to effectively thwart attackers' information, yet limited enough to ensure cost-efficiency. To detect and distinguish changes before and after applying perturbations, a measurement matrix is used [26, 27]. H_t and H'_t represent the measurement matrices before and after the reactance changes, respectively, as formulated in Eq. (27):

$$H = \begin{bmatrix} D_t A^T \\ -D_t A^T \\ A D_t A^T \end{bmatrix}, \quad (27)$$

$$\text{where } D_t = \text{diag}\left(\frac{1}{x_1}, \frac{1}{x_2}, \dots, \frac{1}{x_j}\right)$$

Where D_t is defined as a diagonal matrix where each diagonal element $D_t [j, j]$ equals $\frac{1}{x_j}$, with x_j representing the reactance of branch j . The off-diagonal elements of D_t are set to zero ($D_t [i, j] = 0$ if $i \neq j$), signifying that D_t is a diagonal matrix. Additionally, A^T denotes the transpose of the branch-bus incidence matrix. The elements of A^T take three possible values: 1 if line j originates from bus i , -1 if line j terminates at bus i , and otherwise takes zero. In terms of validation of the proposed model and quantifying its efficiency, the metric η

calculates the detectability of randomly generated attack vectors as defined in Eq. (28).

$$\eta(H, H') = \frac{1}{N} \sum_{i=1}^N \left[\frac{\|H'_t c_i\| - \|H_t c_i\|}{\|H_t c_i\|} \right] \quad (28)$$

Where c_i is the i^{th} randomly generated attack vector, and N is the total number of attack vectors generated which is set to 10,000 attacks. Additionally, $\|H_t c_i\|$ is the projection of c_i onto the measurement space defined by H . The detection percentage depends on the δ which is the detectability threshold. It is common to consider its value more than 50% which is the least level of security.

III. RESULTS AND DISCUSSIONS

1) *System Specifications*: All numerical experiments and simulations in this paper were implemented using Python version 3.12, on a machine with 16 GB RAM and a 12th Gen Intel(R) Core (TM) i7-12650H 2.30 GHz processor. Additionally, the ML-based models were developed using the scikit-learn library [28], while DL-based models were implemented with TensorFlow [29]. Also, to develop the evaluation of the proposed model, a synthetic test system, i.e. Illinois 200-bus, has been taken into account. This system includes overall 37 generators, 200 buses, and 179 lines [30].

2) *Wind-related results*: the results associated with the proposed methods are provided as following. In the data imputation stage, the RF regressor excels other alternatives, so it is used in this paper to accomplish the data recovery task. On this basis, in Fig. 2, the prediction results are shown for different features and timesteps of the training dataset. The considered wind power data sets are related to [31], and 8 features are considered to train our model which are observable in Table I.

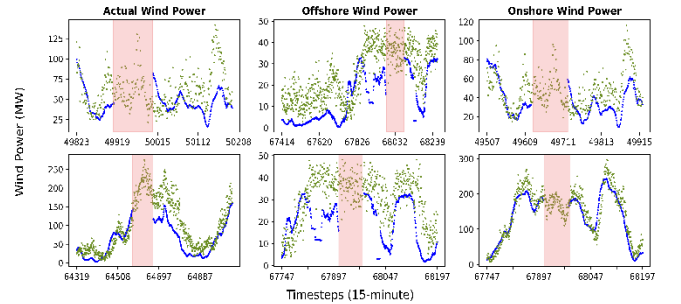


Fig. 2. The prediction results of the RF regressor for three selected features.

In Fig. 2, each red pale area represents a period that related data are missed. Also, blue scatter points show the actual data which are incomplete in specified time intervals. In this way, green scatter points which indicate RF predictions strive to fill the gaps, contributing to implement data recovery. The corresponding time range is from 0 to 201600 (the number of samples or observations is 201600).

TABLE I
PERFORMANCE COMPARISONS OF THREE PREVALENT
REGRESSORS IN THE DATA RECOVERY STAGE

| Regressor | R^2 score |
|---------------------|-------------|
| RF | 0.9504 |
| K-nearest neighbors | 0.7694 |
| HGBR | 0.8574 |

As it was stated, the accurate wind power forecasting is done using augmented BiLSTM model which is equipped by an OPTUNA optimizer. Accordingly, some of the opted parameters by OPTUNA are shown in Table II.

TABLE II
HYPERPARAMETER TUNING RESULTS OBTAINED BY
OPTUNA OPTIMIZER.

| Hyperparameters | Decision space | OPTUNA selected |
|--|----------------------|-----------------|
| $\sigma_{BiLSTM_1}^f, \sigma_{BiLSTM_1}^b$ | [ReLU, Tanh, Linear] | [Tanh, ReLU] |
| $\sigma_{BiLSTM_2}^f, \sigma_{BiLSTM_2}^b$ | [ReLU, Tanh, Linear] | [ReLU, ReLU] |

In this Table, $\sigma_{BiLSTM_1}^f$ and $\sigma_{BiLSTM_2}^f$ present the forward activation functions of the first and second BiLSTM layers. Also, $\sigma_{BiLSTM_1}^b$ and $\sigma_{BiLSTM_2}^b$ point the backward activation functions. In Fig. 3, actual and BiLSTM predicted values for wind power are observable and this figure depicts the wind power forecasting for ten days attained by the modified BiLSTM model. Additionally, in terms of performance evaluation and accuracy, Fig. 4 reveals real and prediction correlations over the time range. As it is obvious, the diagonal clustering shows that the BiLSTM model is effective in predicting wind power with high precision.

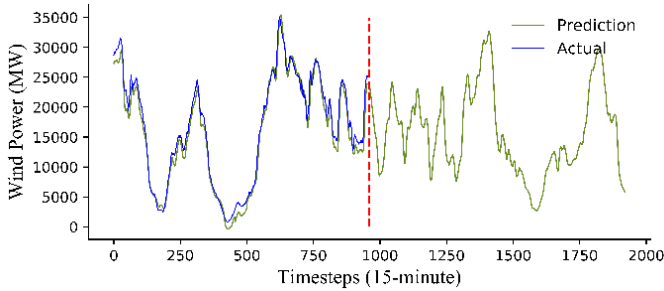


Fig. 3. Wind power prediction used by the proposed modified BiLSTM model for ten days ahead.

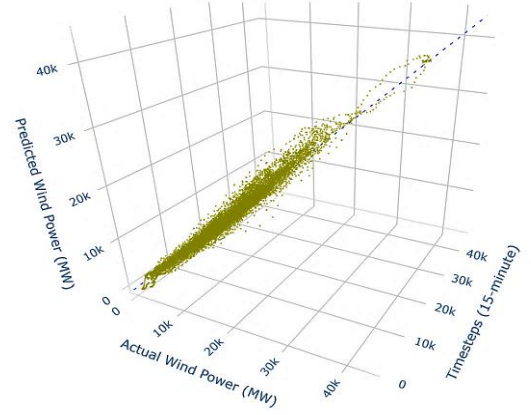


Fig. 4. 3D correlation plot related to the modified BiLSTM predictor.

Four different criteria are employed to assess the performance and delineate the most preferred architecture, gathered in Table III. As it is clear and expected, the proposed modified BiLSTM records much better in comparison with others.

TABLE III
PERFORMANCE MEASURES COMPARISONS BETWEEN THE
PROPOSED MODEL AND SOME OTHER PREVALENT
METHODS

| Evaluation metrics | BiLSTM | LSTM [32] | RNN [33] | GRU [34] |
|--------------------|--------|-----------|----------|----------|
| R^2 | 0.9878 | 0.9808 | 0.9649 | 0.9719 |
| MAPE | 0.1005 | 0.1246 | 0.1559 | 0.1930 |
| NMAE | 1.4284 | 1.7288 | 2.3359 | 2.0894 |
| NRMSE | 1.9385 | 2.4351 | 3.2992 | 2.9511 |

3) *GAN model results:* When the wind power prediction stage is successfully completed by the selected preferable architecture, our proposed ConvGAN model is responsible for estimating wind power fluctuations and uncertainty modeling. As illustrated in Fig. 5, this deep-based generation model must be trained until the generator component can defeat its rival, the discriminator. After training ConvGAN model, it would be able to generate realistic synthetic scenarios. Accordingly, Fig. 5 shows 1000 scenarios generated by the proposed ConvGAN model for a day of wind power prediction.

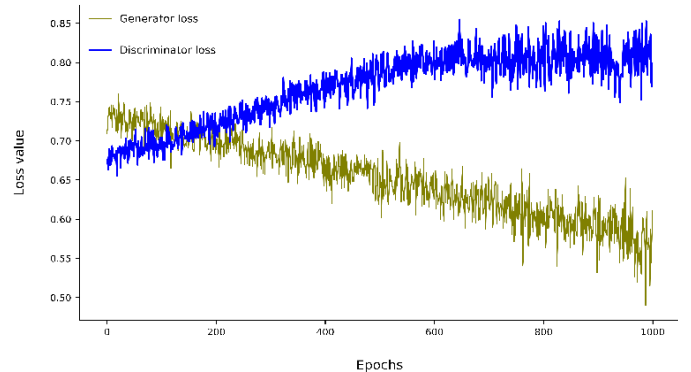


Fig. 5. Fitness process of the proposed ConvGAN model including generator and discriminator during 1000 epochs.

Some other outcomes associated with a thousand generated scenarios by trained GAN model are provided in Fig. 6.

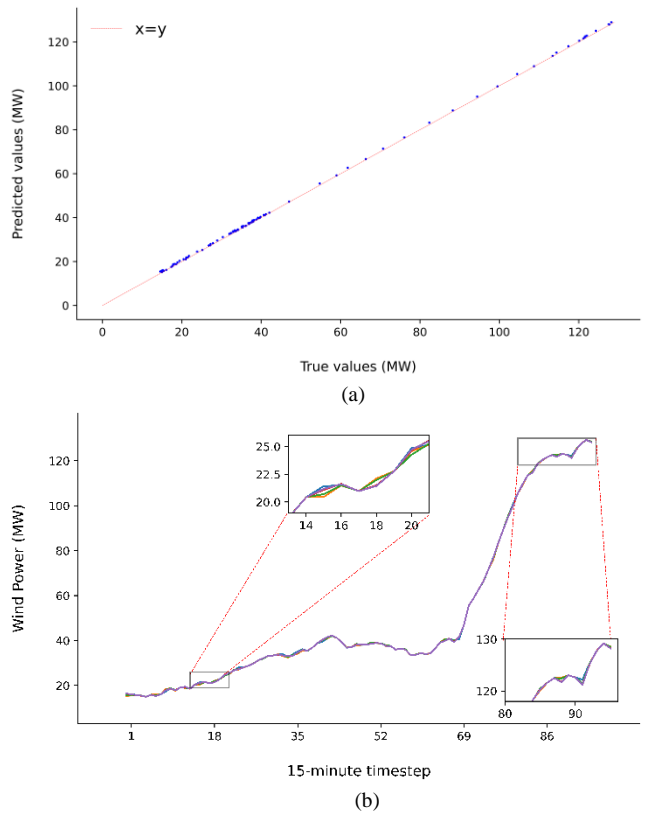


Fig. 6. (a) Correlation curve between the predicted and actual values generated by the ConvGAN model. (b) 1000 randomly generated scenarios of wind power using the ConvGAN model.

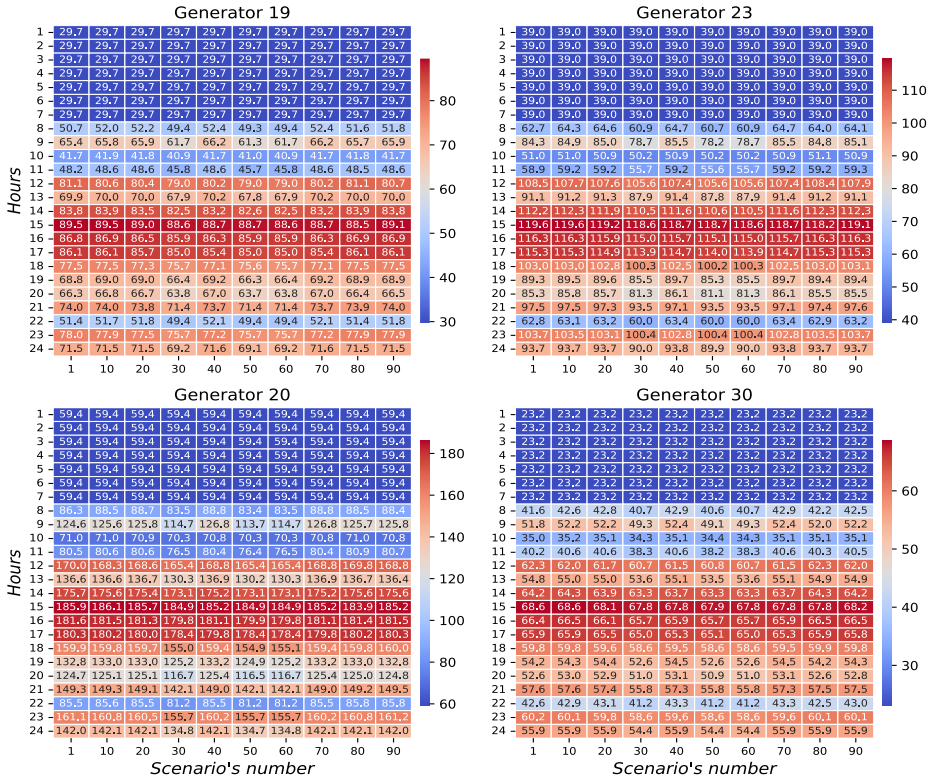


Fig. 7. Cost-benefit optimal scheduling of four sample generators via ten sample scenarios in *Case1*.

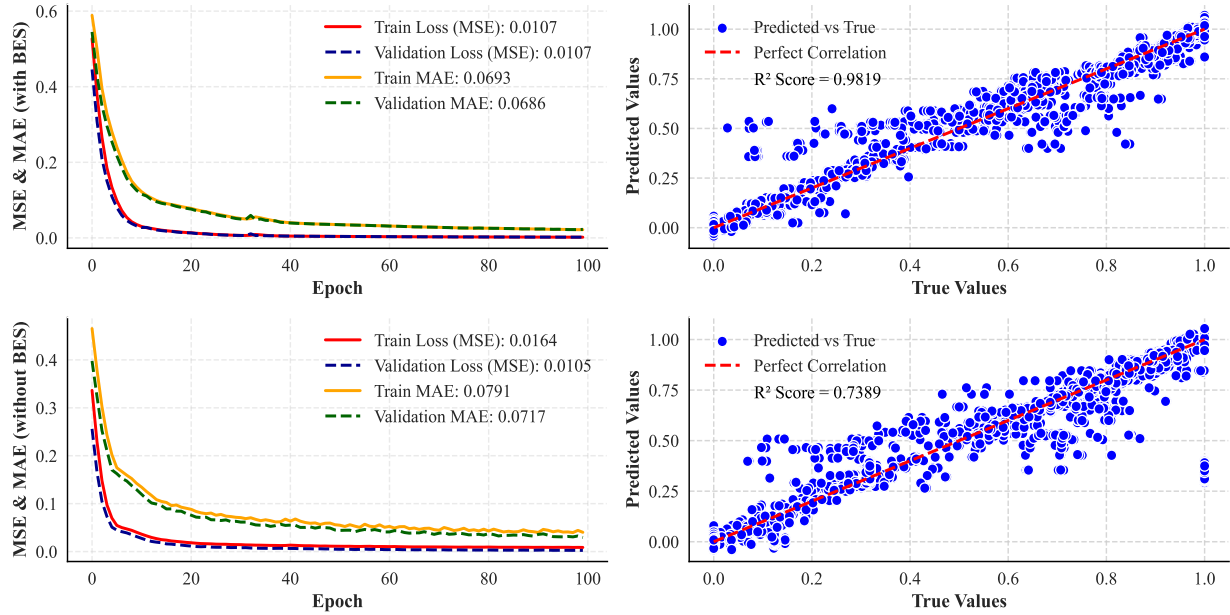


Fig. 8. Fitness evaluation of proposed DeepStack BiLSTM-CNN model along with correlation for both *Case1* & *Case2*.

4) *Predictive optimal scheduling model:* In Fig. 7, the heatmaps illustrate the output scheduling across 10 scenarios for four generators over a 24-hour period. Each color transition from blue to red represents an increase in output level, with blue indicating low output during night hours and red representing peak output hours. The figure highlights the varying operational demands met by each generator, particularly during peak hours (approximately hours 10-19).

This visualization confirms the model's effectiveness in adjusting generator output across scenarios to meet system demands, ensuring economic efficiency and reliability. Fig. 8 illustrates the time-series predictions and correlations for the two cases, achieved using a DeepStack BiLSTM-CNN architecture. As expected, the incorporation of BES leads to reduced operating costs by enhancing wind power integration.

To illustrate this, statistical parameters are presented using box plots, along with their frequency distribution depicted as a violin plot in Fig. 9. These visualizations effectively compare the objective function values for the two cases under discussion. The violin plot highlights the density of the cost values. In both cases, the majority of the costs cluster around their respective medians, with Case 2 showing a more concentrated and narrow distribution due to the stabilizing effect of BES.

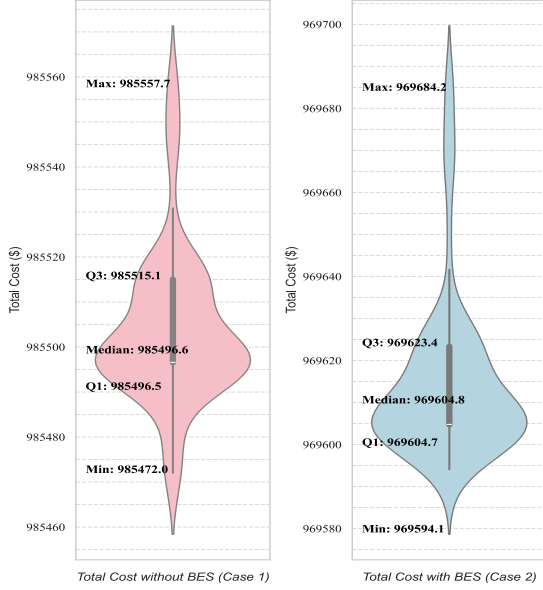


Fig. 9. Fitness evaluation of cost-benefit optimization along with correlation for both Case1 & Case2.

5) *Sensitivity analysis:* With recent technological advancements and economies of scale, BES costs have shown a tendency to decrease, making storage solutions more accessible and economically viable for power systems.

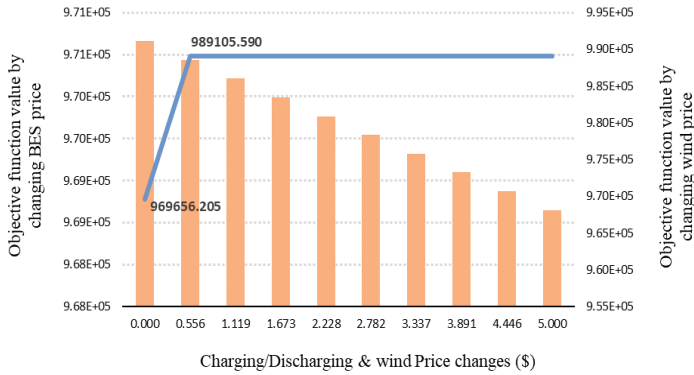


Fig. 10. Evaluating the impacts of BES charging/discharging price along with operating cost of the wind farm on the objective function.

This analysis helps to quantify how fluctuations in BES operational costs, influenced by technological improvements and market dynamics, could impact the overall economic efficiency of the system. Additionally, exploring sensitivity to BES costs provides insights into the cost-benefit trade-offs for grid operators when managing wind power integration and optimizing system loads. As shown in Fig. 10, there is a

continuing reduction in the system's objective function as the operating costs of the BES start to increase. This reflects the fact that higher BES operational costs (charging/discharging) reduce the economic efficiency of using the storage system and make it less attractive for storing excess energy or managing system loads. Moreover, by increasing the operating cost of wind farm, the objective function value increases initially but plateaus at a certain point which indicates that after a certain wind price level, further increases do not impact the objective function.

Given the objective function results in Table IV, along with wind curtailment changes across different scenarios for varying BES sizes and charging/discharging potentials, it can be concluded that investing in larger BES capacities leads to both lower costs and reduced losses. It is important to note that these results are based on the initial BES charging/discharging price, set at $2.5 \frac{\$}{MWh}$.

TABLE IV
THE IMPACTS OF BES SIZE ON THE TOTAL COST AND THE CURTAILED WIND POWER.

| | Objective Function Value (\$) | Wind Curtailment (MW) |
|----------------------------|-------------------------------|-----------------------|
| BES Size (MWh) = 500 | | |
| p_{ch}^{max} (MW) = 250 | 969,652.28 | 102.89 |
| p_{dis}^{max} (MW) = 250 | | |
| BES Size (MWh) = 1000 | | |
| p_{ch}^{max} (MW) = 500 | 955,379.12 | 94.27 |
| p_{dis}^{max} (MW) = 500 | | |
| BES Size (MWh) = 1500 | | |
| p_{dis}^{max} (MW) = 750 | 948,197.74 | 0 |
| p_{ch}^{max} (MW) = 750 | | |

6) *DDM model:* The results related to the cybersecurity-based optimization is provided in this part. In case of 10,000 attacks generated randomly, Fig.11 visualizes how the success rate ($\eta(\delta)$) impacts the incremental cost of DDM (%) for different values of δ , ranging from 0.7 to 0.99. More conservative security filtering (higher δ values) results in a lower ability to reach peak effectiveness. Apart from δ values, the selection of lines and their loadings directly affects effectiveness. In addition to the impacts of the branch network on the objective function, the engagement of BES can also influence the outcomes, which should be considered. Consequently, two scenarios—utilizing BES and not utilizing BES—are conducted, with their detailed results presented in Table V. Although BES utilization does not significantly reduce total costs compared to the economic scheduling mode, in most instances (15 instances), it results in a lower cost increment when compared to scenarios without BES utilization.

IV. CONCLUSION

This paper presents a predictive optimal scheduling framework aimed at reducing wind curtailment by utilizing BES. The proposed predictive model achieved impressive accuracy, with 98.78% precision in wind forecasting and final predictive model's accuracies of 98% and 74% with and without BES integration, respectively.

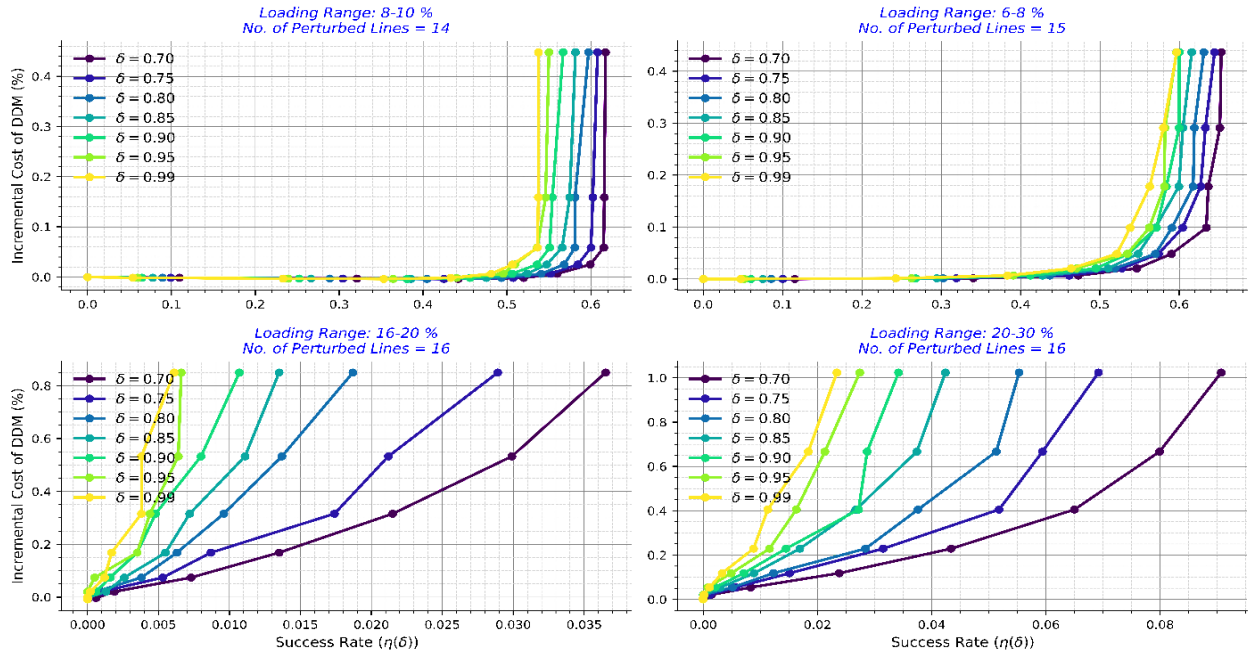


Fig. 11. Trade-off analysis between success rate and incremental cost of DDM across four different loading ranges without using storage.

TABLE V
OPTIMAL COST INCREMENT AND SUCCESS RATE FOR DIFFERENT CASES WITH THEIR CORRESPONDING δ VALUES, DIFFERENTIATED BY CONFIGURATIONS WITH BES AND WITHOUT BES.

| | δ | Optimal Cost Increment | | Optimal Success Rate | | | δ | Optimal Cost Increment | | Optimal Success Rate | |
|-----------------------|----------|------------------------|----------------|----------------------|----------------|-----------------------|----------|------------------------|----------------|----------------------|----------------|
| | | <i>BES</i> | <i>Not BES</i> | <i>BES</i> | <i>Not BES</i> | | | <i>BES</i> | <i>Not BES</i> | <i>BES</i> | <i>Not BES</i> |
| Loading Range: 8-10% | 0.70 | 0.0670 | 0.0650 | 0.3859 | 0.4053 | Loading Range: 6-8% | 0.70 | 0.0242 | 0.0299 | 0.3874 | 0.5326 |
| | 0.75 | 0.0499 | 0.0518 | 0.3859 | 0.4053 | | 0.75 | 0.0212 | 0.0174 | 0.6276 | 0.3155 |
| | 0.80 | 0.0346 | 0.0513 | 0.3859 | 0.6670 | | 0.80 | 0.0121 | 0.0096 | 0.3874 | 0.3155 |
| | 0.85 | 0.0377 | 0.0374 | 0.6321 | 0.6670 | | 0.85 | 0.0099 | 0.0111 | 0.3874 | 0.5326 |
| | 0.90 | 0.0295 | 0.0272 | 0.6321 | 0.4053 | | 0.90 | 0.0094 | 0.0080 | 0.6276 | 0.5326 |
| | 0.95 | 0.0183 | 0.0163 | 0.3859 | 0.4053 | | 0.95 | 0.0031 | 0.0064 | 0.2172 | 0.5326 |
| | 0.99 | 0.0137 | 0.0088 | 0.3859 | 0.2286 | | 0.99 | 0.0044 | 0.0038 | 0.6276 | 0.3155 |
| Loading Range: 16-20% | 0.70 | 0.6099 | 0.6154 | 0.0423 | 0.0585 | Loading Range: 20-30% | 0.70 | 0.6458 | 0.6341 | 0.1878 | 0.0985 |
| | 0.75 | 0.5938 | 0.6002 | 0.0423 | 0.0585 | | 0.75 | 0.6075 | 0.6270 | 0.1026 | 0.1780 |
| | 0.80 | 0.5795 | 0.5810 | 0.0423 | 0.0585 | | 0.80 | 0.6132 | 0.6175 | 0.1878 | 0.1780 |
| | 0.85 | 0.5772 | 0.5658 | 0.1472 | 0.0585 | | 0.85 | 0.5984 | 0.5995 | 0.1878 | 0.1780 |
| | 0.90 | 0.5461 | 0.5509 | 0.0423 | 0.0585 | | 0.90 | 0.5857 | 0.5713 | 0.1878 | 0.0985 |
| | 0.95 | 0.5436 | 0.5361 | 0.0423 | 0.0585 | | 0.95 | 0.5697 | 0.5812 | 0.1878 | 0.1780 |
| | 0.99 | 0.5311 | 0.5364 | 0.0423 | 0.0585 | | 0.99 | 0.5574 | 0.5628 | 0.1878 | 0.1780 |

The results demonstrate that incorporating BES into the power system can obtain lower total costs by at least 1.6% (with minimum storage capacity) and up to 3.78% (with maximum storage capacity). Moreover, wind curtailment was reduced by 5.54% at the lowest and entirely eliminated (100%) at the highest level of utilized BES capacities. Additionally, as detailed in the sensitivity analysis, the impact of three key parameters is explored—which are wind prices and BES charging/discharging costs—on the objective function, providing valuable insights. On this basis, As BES operational costs increase, the economic efficiency of BES diminishes,

making it less attractive for large-scale deployment. Additionally, it is revealed that BES utilization can mitigate the cost increment related to the DDM implementation as well. Furthermore, wind price sensitivity reveals that beyond a certain price threshold, further increases have negligible impact on the objective function, indicating that the optimization model fully leverages wind energy within system constraints.

REFERENCES

- [1] A. A. Eladl *et al.*, "A comprehensive review on wind power spillage: Reasons, minimization techniques, real applications, challenges, and future trends," *Electric Power Systems Research*, vol. 226, p. 109915, 2024.
- [2] H. Chen, J. Chen, G. Han, and Q. Cui, "Winding down the wind power curtailment in China: What made the difference?," *Renewable and Sustainable Energy Reviews*, vol. 167, p. 112725, 2022/10/01/ 2022, doi: <https://doi.org/10.1016/j.rser.2022.112725>.
- [3] W. Zhang, Z. Lin, and X. Liu, "Short-term offshore wind power forecasting-A hybrid model based on Discrete Wavelet Transform (DWT), Seasonal Autoregressive Integrated Moving Average (SARIMA), and deep-learning-based Long Short-Term Memory (LSTM)," *Renewable Energy*, vol. 185, pp. 611-628, 2022.
- [4] R. Zafar and I. Y. Chung, "Data-Driven Multiperiod Optimal Power Flow for Power System Scheduling Considering Renewable Energy Integration," *IEEE Access*, vol. 12, pp. 95278-95290, 2024, doi: 10.1109/ACCESS.2024.3426052.
- [5] A. Peivand, E. Azad Farsani, and H. R. Abdolmohammadi, "Accelerating optimal scheduling prediction in power system: A multi-faceted GAN-assisted prediction framework," *Renewable Energy*, vol. 230, p. 120830, 2024/09/01/ 2024, doi: <https://doi.org/10.1016/j.renene.2024.120830>.
- [6] N. Dkhili *et al.*, "Data-Based Predictive Control for Power Congestion Management in Subtransmission Grids Under Uncertainty," *IEEE Transactions on Control Systems Technology*, vol. 31, no. 5, pp. 2146-2158, 2023, doi: 10.1109/TCST.2023.3291556.
- [7] M. Balci, E. Dokur, U. Yuzgec, and N. Erdogan, "Multiple decomposition-aided long short-term memory network for enhanced short-term wind power forecasting," *IET Renewable Power Generation*, vol. 18, no. 3, pp. 331-347, 2024, doi: <https://doi.org/10.1049/rpg2.12919>.
- [8] O. Abedinia, A. Ghasemi-Marzbali, M. Shafiei, B. Sobhani, G. B. Gharehpetian, and M. Bagheri, "Wind Power Forecasting Enhancement Utilizing Adaptive Quantile Function and CNN-LSTM: A Probabilistic Approach," *IEEE Transactions on Industry Applications*, vol. 60, no. 3, pp. 4446-4457, 2024, doi: 10.1109/TIA.2024.3354218.
- [9] Y. Liu, H. Zhang, P. Guo, C. Li, and S. Wu, "Optimal Scheduling of a Cascade Hydropower Energy Storage System for Solar and Wind Energy Accommodation," *Energies*, vol. 17, no. 11, p. 2734, 2024.
- [10] G. Memarzadeh and F. Keynia, "A new hybrid CBSA-GA optimization method and MRMI-LSTM forecasting algorithm for PV-ESS planning in distribution networks," *Journal of Energy Storage*, vol. 72, p. 108582, 2023/11/30/ 2023, doi: <https://doi.org/10.1016/j.est.2023.108582>.
- [11] J. Li *et al.*, "The state-of-charge predication of lithium-ion battery energy storage system using data-driven machine learning," *Sustainable Energy, Grids and Networks*, vol. 34, p. 101020, 2023/06/01/ 2023, doi: <https://doi.org/10.1016/j.segan.2023.101020>.
- [12] S. M. Nosratabadi *et al.*, "The Impact of Grid Storage on Balancing Costs and Carbon Emissions in Great Britain," *ArXiv*, vol. abs/2410.07740, 2024.
- [13] F. Liu, Q. Liu, Q. Tao, Y. Huang, D. Li, and D. Sidorov, "Deep reinforcement learning based energy storage management strategy considering prediction intervals of wind power," *International Journal of Electrical Power & Energy Systems*, vol. 145, p. 108608, 2023/02/01/ 2023, doi: <https://doi.org/10.1016/j.ijepes.2022.108608>.
- [14] S. Mahjoub, L. Chrifi-Alaoui, S. Drid, and N. Derbel, "Control and implementation of an energy management strategy for a PV-wind-battery microgrid based on an intelligent prediction algorithm of energy production," *Energies*, vol. 16, no. 4, p. 1883, 2023.
- [15] X. Chai, S. Li, and F. Liang, "A novel battery SOC estimation method based on random search optimized LSTM neural network," *Energy*, vol. 306, p. 132583, 2024/10/15/ 2024, doi: <https://doi.org/10.1016/j.energy.2024.132583>.
- [16] N. N. Tran, H. R. Pota, Q. N. Tran, and J. Hu, "Designing Constraint-Based False Data-Injection Attacks Against the Unbalanced Distribution Smart Grids," *IEEE Internet of Things Journal*, vol. 8, no. 11, pp. 9422-9435, 2021, doi: 10.1109/JIOT.2021.3056649.
- [17] M. Ghiasi, T. Niknam, Z. Wang, M. Mehrandezh, M. Dehghani, and N. Ghadimi, "A comprehensive review of cyber-attacks and defense mechanisms for improving security in smart grid energy systems: Past, present and future," *Electric Power Systems Research*, vol. 215, p. 108975, 2023/02/01/ 2023, doi: <https://doi.org/10.1016/j.eprsr.2022.108975>.
- [18] S. Lakshminarayana and D. K. Y. Yau, "Cost-Benefit Analysis of Moving-Target Defense in Power Grids," *IEEE Transactions on Power Systems*, vol. 36, no. 2, pp. 1152-1163, 2021, doi: 10.1109/TPWRS.2020.3010365.
- [19] N. Kharlamova, S. Hashemi, and C. Træholt, "Data-driven approaches for cyber defense of battery energy storage systems," *Energy and AI*, vol. 5, p. 100095, 2021/09/01/ 2021, doi: <https://doi.org/10.1016/j.egyai.2021.100095>.
- [20] B. L.-M. Learn, "Random forest," vol. vol. 45, 2001.
- [21] M. Xia, H. Shao, X. Ma, and C. W. de Silva, "A stacked GRU-RNN-based approach for predicting renewable energy and electricity load for smart grid operation," *IEEE Transactions on Industrial Informatics*, vol. 17, no. 10, pp. 7050-7059, 2021.
- [22] W. Liao, S. Wang, B. Bak-Jensen, J. R. Pillai, Z. Yang, and K. Liu, "Ultra-Short-Term Interval Prediction of Wind Power Based on Graph Neural Network and Improved Bootstrap Technique," *Journal of Modern Power Systems and Clean Energy*, 2023.
- [23] K. L. M. -S. Ko, J. -K. Kim, C. W. Hong, Z. Y. Dong and K. Hur, "Deep Concatenated Residual Network With Bidirectional LSTM for One-Hour-Ahead Wind Power Forecasting," in *IEEE Transactions on Sustainable Energy*, vol. 12, no. 2, pp. 1321-1335, April 2021, doi: 10.1109/TSST.2020.3043884.
- [24] T. Akiba, S. Sano, T. Yanase, T. Ohta, and M. Koyama, "Optuna: A next-generation hyperparameter optimization framework," in *Proceedings of the 25th ACM SIGKDD international conference on knowledge discovery & data mining*, 2019, pp. 2623-2631.
- [25] X. Zhang, D. Li, and X. Fu, "A novel Wasserstein generative adversarial network for stochastic wind power output scenario generation," *IET Renewable Power Generation*, 2024.
- [26] B. Liu and H. Wu, "Optimal Planning and Operation of Hidden Moving Target Defense for Maximal Detection Effectiveness," *IEEE Transactions on Smart Grid*, vol. 12, no. 5, pp. 4447-4459, 2021, doi: 10.1109/TSG.2021.3076824.
- [27] W. Xu, I. M. Jaimoukha, and F. Teng, "Robust moving target defence against false data injection attacks in power grids," *IEEE Transactions on Information Forensics and Security*, vol. 18, pp. 29-40, 2022.
- [28] O. Kramer and O. Kramer, "Scikit-learn," *Machine learning for evolution strategies*, pp. 45-53, 2016.
- [29] M. Abadi *et al.*, "TensorFlow: Large-Scale Machine Learning on Heterogeneous Distributed Systems," *ArXiv*, vol. abs/1603.04467, 2016.
- [30] A. B. Birchfield, T. Xu, K. M. Gegner, K. S. Shetye, and T. J. Overbye, "Grid structural characteristics as validation criteria for synthetic networks," *IEEE Transactions on power systems*, vol. 32, no. 4, pp. 3258-3265, 2016.
- [31] *Open Power System Data*, doi: https://doi.org/10.25832/time_series/2020-10-06.
- [32] S. Siami-Namini, N. Tavakoli, and A. S. Namin, "The Performance of LSTM and BiLSTM in Forecasting Time Series," in *2019 IEEE International Conference on Big Data (Big Data)*, 9-12 Dec. 2019 2019, pp. 3285-3292, doi: 10.1109/BigData47090.2019.9005997.
- [33] S. Narayanan, R. Kumar, S. Ramadass, and J. Ramasamy, "Hybrid Forecasting Model Integrating RNN-LSTM for Renewable Energy Production," *Electric Power Components and Systems*, pp. 1-19, 2024.
- [34] S. Zhang, E. Robinson, and M. Basu, "Wind power forecasting based on a novel gated recurrent neural network model," *Wind Energy and Engineering Research*, vol. 1, p. 100004, 2024/08/01/ 2024, doi: <https://doi.org/10.1016/j.weer.2024.100004>.



Ali Peivand received his B.S. degree in Electrical Engineering from the Sirjan University of Technology, Sirjan, Iran, in 2016, and the M.S. degree in Power Systems Engineering from the Isfahan University of Technology, Isfahan, Iran, in 2024. His research interests include

power system analysis and modeling, smart grids, optimization, and renewable energy resources. He has authored several peer-reviewed papers focused on the integration of renewable energy sources into the power grid and the application of optimization techniques in smart grids. His scholarly work aims to advance the efficiency and sustainability of power systems through cutting-edge research.



Seyyed Mostafa Nosratabadi (Member, IEEE) received the Ph.D. degree from University of Isfahan, Isfahan, Iran, in 2016, all in electrical engineering. Since 2016 to 2022, he has been an Assistant Professor at the Department of Electrical Engineering, Sirjan University of

Technology, Sirjan, Iran. From 2022, he has been Research Associate at the University of Edinburgh, UK and the University of Oxford, UK for two years and he has been a member of EPSRC funded project. Currently, he is a Research Fellow at the College of Engineering and Physical Sciences, University of Birmingham, UK. He has published over 50 journal and conference papers. His research interests are power and energy systems modeling, operation & optimization, energy markets and smart grids.